Hindawi Publishing Corporation
Journal of Nanomaterials
Volume 2013, Article ID 654716, 6 pages
http://dx.doi.org/10.1155/2013/654716

Research Article

Durability of LDPE Nanocomposites with Clay, Silica, and Zinc Oxide—Part I: Mechanical Properties of the Nanocomposite Materials

Halim Hamid Redhwi,[1] Mohammad Nahid Siddiqui,[2] Anthony L. Andrady,[3] and Syed Hussain[4]

[1] *Chemical Engineering Department, King Fahd University of Petroleum & Minerals, Dhahran 31261, Saudi Arabia*
[2] *Chemistry Department and Center of Excellence in Nanotechnology (CENT), King Fahd University of Petroleum & Minerals, Dhahran 31261, Saudi Arabia*
[3] *Department of Chemical and Biomolecular Engineering, North Carolina State University, Raleigh, NC 27607, USA*
[4] *Dhahran Techno-Valley, King Fahd University of Petroleum & Minerals, Dhahran 31261, Saudi Arabia*

Correspondence should be addressed to Halim Hamid Redhwi; hhamid@kfupm.edu.sa

Received 12 January 2013; Revised 26 February 2013; Accepted 28 February 2013

Academic Editor: Jinquan Wei

Three types of LDPE-based nanocomposites with montmorillonite clay, silica, and zinc oxide were prepared by melt blending the nanofiller with the resin. As a prelude to studying their durability, the extent of reinforcement of the LDPE matrix by the nanofillers was investigated using mechanical, thermal, and microscopic studies of the composites. No significant chemical modification of the polyethylene matrix was observed as a result of the processing of the composite compound. While reinforcement was obtained in all cases, the efficiency of reinforcement appears to be qualitatively influenced by surface functionalization, filler interactions, and the extent of dispersion of the filler in the matrix as well as the specific surface area of the nanoparticle fillers.

1. Introduction

Reinforcing fillers are commonly used in polymer formulations to improve the modulus and other mechanical properties of the material. It is the interaction of the filler particle surface with the plastic matrix and the ensuing formation of an interfacial layer that yields the anticipated improvement of properties. Therefore, decrease in average particle size of fillers and the consequent increase in specific surface area are desirable in designing better composites, as it increases the polymer/nanofiller interfacial volume. Thermoplastic nanocomposites often show superior mechanical properties compared to the conventional composites at a lower loading of the filler.

Using nanoscale fillers can also improve the weatherability of nanocomposites by providing more efficient light shielding by the filler particles during outdoor exposure. Higher specific surface area of nanofiller results in more efficient shielding of underlying polymer matrix compared to conventional fillers at the same volume fraction.

Superior weatherability of PP/ZnO nanocomposites [1] and PP/double hydroxide nanocomposites [2] has been reported. Rutile-based nanocomposites of polyurethane [3] and poly (methyl methacrylate) [4] also show markedly improved weatherability. nanocomposite coatings with ZnO used as a protective lacquer on pine wood surface afforded a level of stabilization superior to that afforded by even conventional UV absorbers or the hindered-amine light stabilizers (HALSs) [5]. However, in clay-based systems such as PP/montmorillonite (MMT), the weatherability of the nanocomposite was poorer compared to the unfilled

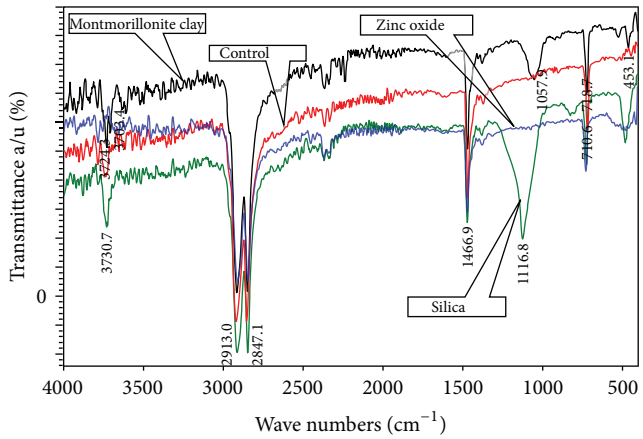

FIGURE 1: Overlay of FT-IR spectra of the LDPE control and nanocomposite samples.

PP matrix [6, 7]. A similar observation was reported for polyethylene as well [8].

The most widely used thermoplastic polyethylene is a good matrix polymer for use in low-cost nanocomposite design. In the laboratory, polymerization in the presence of nanofiller has been used successfully to produce such composites. Alexandre et al. [9] reported the synthesis of polyethylene-layered silicate nanocomposites by this technique. Others have reported the preparation of PE/clay hybrid [10] as well as PE/Silica nanocomposites [11] using a similar approach. Both the low-density polyethylene (LDPE) [12, 13], as well as polypropylene, and nanocomposites reinforced with clay [14, 15] have also been reported using the same method. Chemical modification of the polymer to increase the matrix-resin compatibility often helps in dispersion of the nanofillers. Wang et al. [16, 17], for instance, grafted polar monomer maleic anhydride to the backbone of polyethylene via to prepare (LLDPE-MAH)/clay nanocomposites.

However, in commercial production of composites, in situ polymerization is neither practical nor cost-effective, and melt mixing in conventional processing machinery such as Brabender and compounding extruders will be used. Melt blending of clay and silica with polyethylene can be successfully achieved [18, 19]. However, it is critical to obtain full dispersion of filler to ensure the largest improvement in mechanical properties of the nanocomposite. Sanchez-Valdes et al. [20], for instance, studied the polyethylene/MMT blends. nanocomposite films of LDPE were prepared by melt blending in that study. A grade of low-density polyethylene (LDPE) grafted with maleic anhydride (LDPE-g-MA) was used as a compatibilizer to ensure full dispersion.

In this study, we compare nanocomposites of LDPE obtained at constant weight fraction of three fillers with very different characteristics. Smectite clay (MMT) is made of tactoids of nanoscale plates; fumed silica is hydrophilic filler that tends to form a 3D network by hydrogen-bonded association, and zinc oxide is spherical oxide filler.

Part I of the paper addresses the mechanical characteristics of the nanocomposite, and Part II will be on the weatherability of the nanocomposite materials under outdoor and accelerated weathering exposure.

2. Experimental

The LDPE used in the study was ExxonMobil LDPE LD 160AT, an injection-molding grade of resin with a melt flow index of 4 (g/10 m.). Three nanoscale fillers were commercially procured and used as received: MMT clay cloisite 20A (Nanocor, Hoffman Estates, IL, USA), zinc oxide (Advanced Materials, Manchester, CT, USA), nanosilica Aerosil OX 50 (Evonik, Addison, IL, USA). Cloisite 20 is natural montmorillonite clay modified with a quaternary ammonium salt. The specific surface areas of the fillers used, according to the manufacturers, are as follows: cloisite 20 = 10.9 sq.m./g. [21]; nanosilica = 50 sq.m./g; nanozinc oxide = 35 sq.m./g.

A Theyson TSK 21 mm Twin Screw extruder was used to melt compound the nanofillers into the plastic resin at a level of 5 wt% of the filler. The screw rpm was controlled at 215–218 during extrusion, and the melt temperature was maintained in the range of 375°F to 401°F (190 to 205°C). The compounded resin was pelletized and stored dry for molding. Injection molding of the ASTM test pieces was carried out on a 165 ton Engel machine at a nozzle temperature of 420 F (215°C) and an injection pressure of 5000 psi. Test pieces were stored in the dark at ambient temperature until testing and/or exposure experiments.

Tensile testing was carried out according to ASTM D 638 using Instron Tensile Testing machine, Model 3367. Tests were conducted at room temperature (20 to 22°C) at a strain rate of 10 mm/min. Load displacement data were recorded digitally on a computer attached with the machine.

Microstructural characterization was carried out using Scanning Electron Microscope, Model JEOL JSM-6064LV. The micrographs were taken at 15 kV accelerating voltage and at various magnifications of ×200, ×500, and ×2000. A Mettler Toledo Model DSC 822 Model Differential Scanning Calorimeter: DSC 822 was used to find glass transition temperature and exothermic crosslinking reactions of the test samples exposed to different environmental conditions. Typically, the samples were heated from room temperature to 170 and 300°C, respectively, at a heating rate of 10°C/min under nitrogen flow. Melting temperature is detected as the peak temperature, and the melting heat is obtained from the area of the peak after the baseline correction.

Infrared spectra (IR) were recorded on a Perkin Elmer Model 16F PC FT-IR spectrophotometer loaded with Spectrum v2.00 software (Mass, USA). ATR IR spectra of various polymers were run. All IR spectra of samples were recorded in the range of 400–4000 cm^{-1}.

3. Results and Discussion

Incorporation of the nanofillers into the LDPE even at the 5 wt% level results only in small changes in the FT-IR spectra of composites. Incorporating the filler generally does not chemically alter the polymer, and large changes in the infrared spectra are not anticipated. An overlay of the FT-IR spectra for the different composites shown in Figure 1 is consistent with this expectation. However, comparing the FTIR spectrum of LDPE-ZnO nanocomposite with the control LDPE sample, the absorption band at 2364 cm^{-1}

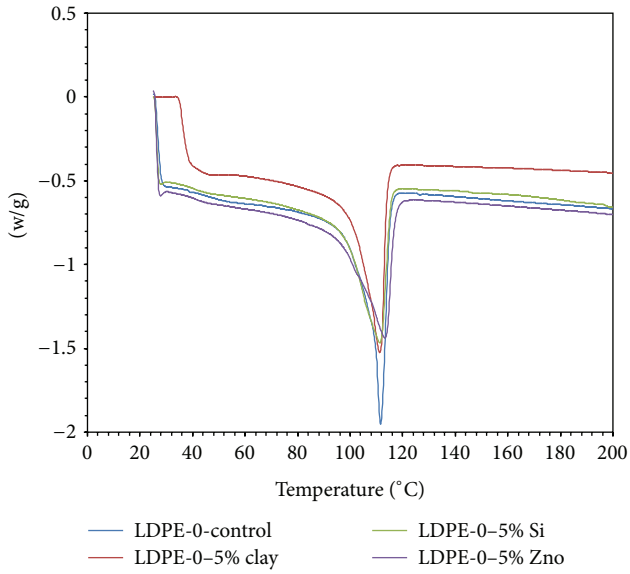

Figure 2: Differential scanning calorimetry for the different nanocomposite compositions, shown overlaid to illustrate the lack of any significant difference in the crystalline melt temperatures.

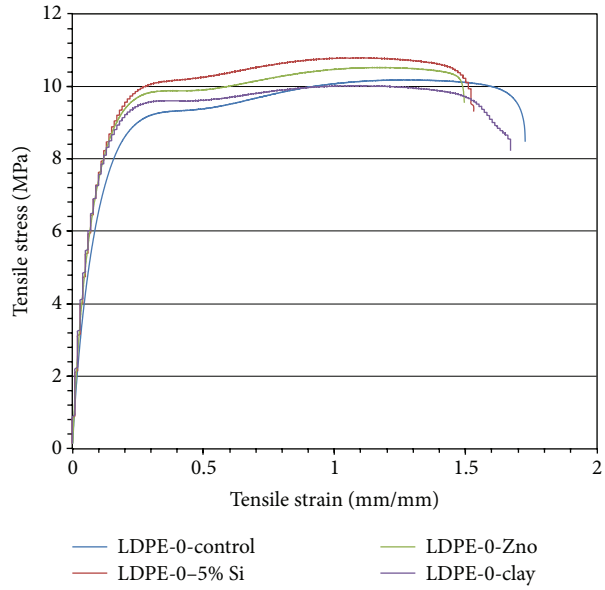

Figure 3: Plot of tensile stress versus tensile strain for LDPE control sample, LDPE-5 wt% nano-SiO_2 sample, LDPE-5 wt% nano-ZnO sample, and LDPE-5 wt% nanoclay sample.

appears to be more intense in the former spectrum. This peak is generally attributed to sorbed CO_2 on the nanoparticles. Also a new peak at about 500 cm^{-1} is apparent; this is likely from prismatic microstructure of the filler [22] that obtains a peak at 512 cm^{-1}.

With LDPE-nano-SiO_2 nanocomposite, the peak at 3730 cm^{-1} is more intense probably due to the contribution of O–H groups in the silica filler that was incorporated. The fundamental silica powder vibration band is seen as an intense peak at 1117 cm^{-1}. LDPE-MMT nanocomposite shows two sharp and intense peaks at 3724 and 3703 cm^{-1}, which are likely due to the N–H functional groups in the amine-functionalized clay.

The DSC studies of crystalline melting cycles did not show any significant differences between the thermal behaviors of the nanocomposites as shown in Figure 2, where the exemplary thermograms are overlaid. In each case, during the first heating, the melting started early to yield a peak at about 112–113°C. The lack of a significant difference in the thermal characteristics of LDPE nanocomposites is in contrast to that of HDPE [13, 16, 17] and PP [23] nanocomposites. In these instances, the change in thermal behavior was attributed to increased nucleation facilitated by the nanoclay particles. Both HDPE and PP are more readily crystallizable compared to LDPE, and presence of MMT is not expected to result in a significant increase in nucleation in the present composites. Our finding is consistent with previously reported data on LDPE/clay nanocomposites with a much higher (~30 wt percent) of the clay [24]. The minimal change in the thermal behavior of present nanocomposites is primarily because of the minimal volume fraction of nanofiller used in these compositions and the consequent small fraction of interfacial volume created in the composite.

Fillers mostly affect the mechanical properties of the polymer matrix. Figure 3 shows typical data for the different composites. Observed deformations of the test pieces were uniform along the gauge length at strains up to the yield point. Thereafter, a neck was formed in the test piece, and further deformation was localized in this region, which expanded in length with further strain.

The shapes of the tensile curves remained the same despite differences in type of fillers and variations in the volume fraction. The tensile extensibility also appears to be not drastically affected by filler type used; it is about 10% less than that for the unfilled LDPE. The tensile modulus, however, is a particularly sensitive metric of the degree of reinforcement achieved in the LDPE nanocomposites. As shown in Table 1, the average modulus of LDPE increased from the base value of 35.4 MPa by about 150% for composites with nano-ZnO, 150% for the MMT clay, and 25% for nanosilica.

The efficiency of reinforcement of a plastic matrix by filler can be quantified using a simple expression [25] that assumes a homogeneous structure with no orientation effects. Using nominal density (g/cm^3) for the density of each filler (clay = 1.8; ZnO = 5.6; SiO_2 = 2.1), a value of volume fraction of p corresponding to 5 weight percent filler was calculated and used in the following [25]:

$$\text{Efficiency} = \frac{\{E_C - (1-p)\,E_O\}}{p}, \tag{1}$$

where E_C = modulus of the composite; E_O = modulus of unfilled polymer, and p = volume fraction of the filler.

As the weight fraction of filler was constant at 0.05, the efficiency invariably being proportional to the surface area should decrease with increasing density of filler. However, this assumes the particle size of filler and the level of dispersion of the filler in the matrix to be the same for all cases. Average primary particle sizes of fillers as suggested

Table 1: Summary of tensile data for the control sample and three composites of LDPE.

Material	Property	Sample Identification						Average	Std. Dev.
		Sample no. 1	Sample no. 2	Sample no. 3	Sample no. 4	Sample no. 5	Sample no. 6		
LDPE control	Maximum load, N	388.98	387.85	388.16	386.68	388.38	401.09	390.19	5.39
	Tensile strength, Mpa	10.18	10.12	10.15	10.12	10.17	10.49	10.21	0.14
	% elongation at break	172.84	164.63	169.24	174.01	179.38	172.59	172.12	4.93
	Modulus of elasticity, MPa	36.06	35.69	35.24	34.39	34.96	35.95	35.38	0.64
LDPE 5 wt% ZnO	Maximum load, N	404.31	404.51	405.92	405.73	402.1	403.6	404.36	1.42
	Tensile strength, Mpa	10.54	10.59	10.54	10.5	10.53	10.52	10.54	0.03
	% elongation at break	155.12	160.03	165.29	161.83	149.41	165.15	159.47	6.20
	Modulus of elasticity, MPa	89.99	89.03	90.13	86.47	90.12	89.32	89.18	1.40
LDPE 5 wt% SiO_2	Maximum load, N	418.05	416.58	416.72	417.56	417.84	413.94	416.78	1.51
	Tensile strength, Mpa	10.79	10.64	10.74	10.85	10.79	10.65	10.74	0.08
	% elongation at break	152.53	152.24	153.74	154.82	155.45	154.37	153.86	1.27
	Modulus of elasticity, MPa	44.34	43.95	43.05	45.25	44.56	44.13	44.21	0.73
LDPE 5 wt% clay	Maximum load, N	392.38	388.16	387.44	391.7	389.67	389.5	389.81	1.93
	Tensile strength, Mpa	10.20	10.56	10.45	10.02	10.15	9.89	10.21	0.25
	% elongation at break	168.92	167.94	171.62	167.06	170.65	167.8	169.00	1.78
	Modulus of elasticity, MPa	88.72	91.7	91.73	86.85	89.93	90.48	89.90	1.88

Table 2: Summary of nanocomposite characteristics.

Filler	Density (g/cc)	p^*	{ΔModulus/p} GPa	Nominal BET values (sq.m./g)
MMT clay	2.86	0.027	1.99	750
Zinc oxide	5.6	0.009	0.98	35
Silica	2.1	0.023	2.37	~50

$^*p$ is the volume fraction of the filler.

by the manufacturer-supplied BET data (see Table 2) are very different. Table 2 lists the observed reinforcement efficiencies calculated as the increase in modulus per unit volume fraction of filler. The efficiencies predicted by (1) for different fillers are not proportional to the filler volume fraction or specific surface area. The highest efficiency of reinforcement (6.0 GPa) is obtained with ZnO, which has the smallest BET area.

The observed efficiency of reinforcement (Table 2) {Δ Modulus/p} decreased in the order Silica > MMT Clay > ZnO. Simple expressions such as (1) fail to predict even this order, as they do not take into account geometric factors such as the aspect ratio and assume a complete dispersion of the nanoparticles. Both MMT clay and nanosilica yielded efficiencies of reinforcement that are disproportionately higher than predicted by (1).

The MMT clay sample with a high BET value (i.e., 750 sq.m./g) is chemically modified with a quaternary amine with long hydrocarbon chains. These render the clay nanofiller particles hydrophobic and compatible with the LDPE matrix. The high reinforcing efficiency of MMT clay filler relative to silica is likely due to its unique surface chemistry. The interphase characteristics that determine reinforcement depend strongly on surface functionality of the filler. Hydrophobic surfaces tend to facilitate stronger matrix-filler bonding with polyethylene.

With nanosilica, however, strong hydrogen-bonded interaction [26], via the silanol groups (Si–OH) on the nanoparticle surface, is expected (band around 3700 cm^{-1} in the FT-IR spectrum due to the silanol groups). This agglomeration yields a 3-dimensional silica network structure that is particularly efficient in reinforcing.

All nanocomposites show the same average tensile strength compared to that of LDPE. This is not unexpected as large changes in tensile strength and extensibility cannot be expected at a loading of only 5 wt.% of nanofiller.

The results show that in addition to filler-matrix interactions, the dispersion of filler in the matrix also must be taken into account in assessing relative efficiencies of reinforcement.

Figure 4 shows SEM images at a magnification of ×2000 that show no obvious signs of agglomeration of the filler. At this magnification, significant agglomeration should be discernible. While some idea of the level of dispersion might be ascertained by scanning electron microscopy (SEM), the small areas sampled by this technique do not yield an average picture of the sample. Also, transmission electron microscopy (TEM) is better suited than SEM for studying nanoparticle dispersion.

4. Conclusions

All three nanoscale fillers melt-blended into LDPE resulted in the reinforcement of the matrix. The observed efficiency

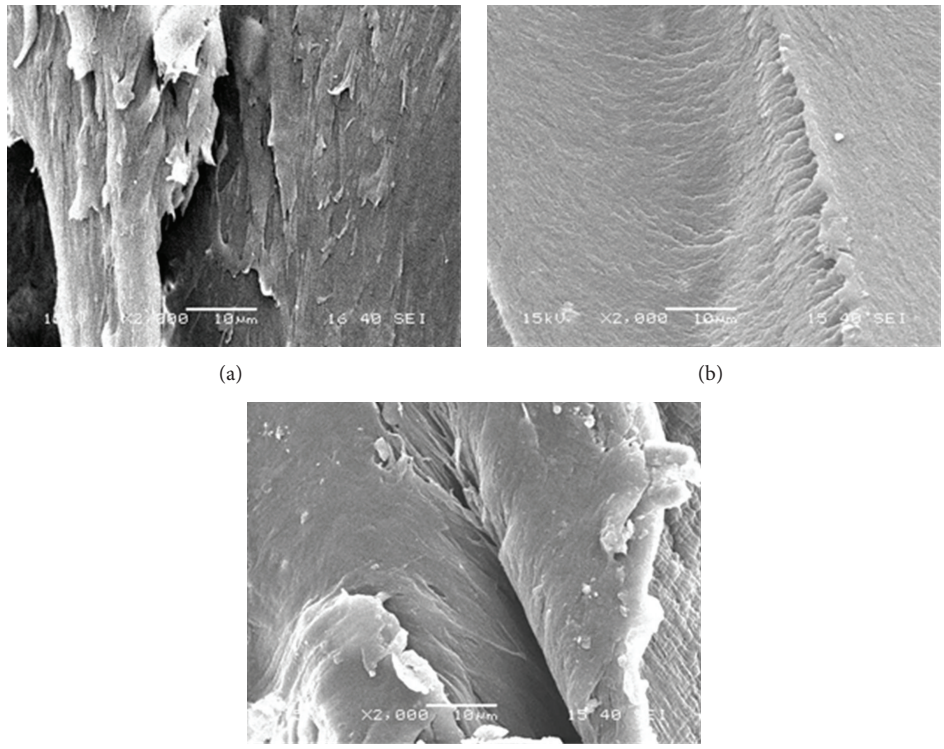

(a) (b)

(c)

Figure 4: Scanning electron micrograph of nanocomposite samples at ×2000 magnification (a) LDPE-5 wt%-ZnO sample, (b) LDPE-5 wt%-SiO_2 sample, and (c) LDPE-5 wt%-clay sample.

of reinforcement by the nanofillers decreased in the order Silica > MMT Clay > ZnO. This order cannot be predicted on the basis of simple models of reinforcement. While the specific surface area of fillers is an important factor, others such as particle geometry, chemical modifications, and potential for ordering into 3-dimensional networks (in the case of silica) also influence reinforcement. In predicting reinforcement, these other factors as well as the efficiency of dispersion need to be taken into account.

Acknowledgment

The authors would like to acknowledge the support provided by the Deanship of Scientific Research (DSR) at King Fahd University of Petroleum and Minerals (KFUPM), Dhahran, Saudi Arabia, for funding this work through Project no. IN100021.

References

[1] H. Zao and R. K. Y. Li, "A study on the photo-degradation of zinc oxide (ZnO) filled polypropylene nanocomposites," *Polymer*, vol. 47, no. 9, pp. 3207–3217, 2006.

[2] D. Peng and B. Qu, "Synthesis of exfoliated PP/LDH nanocomposites via melt-intercalation: structure, thermal properties, and photo-oxidative behavior in comparison with PP/MMT nanocomposites," *Polymer Engineering and Science*, vol. 46, no. 9, pp. 1153–1159, 2006.

[3] X. D. Chen, Z. Wang, Z. F. Liao, Y. L. Mai, and M. Q. Zhang, "Roles of anatase and rutile TiO_2 nanoparticles in photooxidation of polyurethane," *Polymer Testing*, vol. 26, no. 2, pp. 202–208, 2007.

[4] L. Zan, Z. Liu, W. Fa, and T. Peng, "Novel polymethyl methacrylate (PMMA) TiO_2 nanocomposite and its thermal and photic stability," *Wuhan University Journal of Natural Sciences*, vol. 11, no. 2, pp. 415–418, 2006.

[5] F. Weichelt, R. Emmler, R. Flyunt, B. Beyer, M. R. Buchmeiser, and M. Beyer, "ZnO-based UV nanocomposites for wood coatings in outdoor applications," *Macromolecular Materials and Engineering*, vol. 295, no. 2, pp. 130–136, 2009.

[6] S. Chmela, A. Kleinova, A. Fiedlerova et al., "Photo-oxidation of sPP/organoclay nanocomposites," *Journal of Macromolecular Science A*, vol. 42, no. 7, pp. 821–829, 2005.

[7] H. Qin, S. Zhang, H. Liu, S. Xie, M. Yang, and D. Shen, "Photo-oxidative degradation of polypropylene/montmorillonite nanocomposites," *Polymer*, vol. 46, no. 9, pp. 3149–3156, 2005.

[8] A. P. Kumar, D. Depan, N. S. Tomer, and R. P. Singh, "Nanoscale particles for polymer degradation and stabilization-trends and future perspectives," *Progress in Polymer Science*, vol. 34, no. 6, pp. 479–515, 2009.

[9] M. Alexandre, P. Dubois, T. Sun, J. M. Garces, and R. Jérôme, "Polyethylene-layered silicate nanocomposites prepared by the polymerization-filling technique: synthesis and mechanical properties," *Polymer*, vol. 43, no. 8, pp. 2123–2132, 2002.

[10] S. Y. A. Shin, L. C. Simon, J. B. P. Soares, and G. Scholz, "Polyethylene-clay hybrid nanocomposites: in situ polymerization using bifunctional organic modifiers," *Polymer*, vol. 44, no. 18, pp. 5317–5321, 2003.

[11] W. Cheng, W. Miao, J. Peng, W. Zou, and L. Zhang, "Synthesis of silica/polyolefin nanocomposites via two-step method," *Iranian Polymer Journal*, vol. 18, no. 5, pp. 365–371, 2009.

[12] J. Zhang and C. A. Wilkie, "Preparation and flammability properties of polyethylene-clay nanocomposites," *Polymer Degradation and Stability*, vol. 80, no. 1, pp. 163–169, 2003.

[13] T. G. Gopakumar, J. A. Lee, M. Kontopoulou, and J. S. Parent, "Influence of clay exfoliation on the physical properties of montmorillonite/polyethylene composites," *Polymer*, vol. 43, no. 20, pp. 5483–5491, 2002.

[14] P. H. Nam, P. Maiti, M. Okamoto, T. Kotaka, N. Hasegawa, and A. Usuki, "A hierarchical structure and properties of intercalated polypropylene/clay nanocomposites," *Polymer*, vol. 42, no. 23, pp. 9633–9640, 2001.

[15] M. Kawasumi, N. Hasegawa, M. Kato, A. Usuki, and A. Okada, "Preparation and mechanical properties of polypropylene-clay hybrids," *Macromolecules*, vol. 30, no. 20, pp. 6333–6338, 1997.

[16] K. H. Wang, M. H. Choi, C. M. Koo, M. Z. Xu, I. J. Chung, and M. C. Jang, "Morphology and physical properties of polyethylene/silicate nanocomposite prepared by melt intercalation," *Journal of Polymer Science B*, vol. 40, no. 14, pp. 1454–1463, 2002.

[17] K. H. Wang, I. J. Chung, M. C. Jang, J. K. Keum, and H. H. Song, "Deformation behavior of polyethylene/silicate nanocomposites as studied by real-time wide-angle X-ray scattering," *Macromolecules*, vol. 35, no. 14, pp. 5529–5535, 2002.

[18] L. Wei, T. Tang, and B. Huang, "Synthesis and characterization of polyethylene/clay-silica nanocomposites: a montmorillonite/silica-hybrid-supported catalyst and in situ polymerization," *Journal of Polymer Science A*, vol. 42, no. 4, pp. 941–949, 2004.

[19] M. Q. Zhang, M. Z. Rong, H. B. Zhang, and K. Friedrich, "Mechanical properties of low nano-silica filled high density polyethylene composites," *Polymer Engineering and Science*, vol. 43, no. 2, pp. 490–500, 2003.

[20] S. Sanchez-Valdes, M. L. Lopez-Quintanilla, E. Ramirez-Vargas et al., "Effect of ionomeric compatibilizer on clay dispersion in polyethylene/clay nanocomposites," *Macromolecular Materials and Engineering*, vol. 291, no. 2, pp. 128–136, 2006.

[21] T. V. González, C. G. Salazar, J. R. D. Rosa, and V. G. González, "Nylon 6/organoclay nanocomposites by extrusion," *Journal of Applied Polymer Science*, vol. 108, no. 5, pp. 2923–2933, 2008.

[22] H. Abdullah, N. P. Ariyanto, S. Shaari, B. Yuliarto, and S. Junaidi, "TEC and scintillation study of equatorial ionosphere: a month campaign over Sipitang and Parit Raja Stations, Malaysia," *American Journal of Engineering and Applied Sciences*, vol. 2, no. 1, pp. 236–240, 2009.

[23] R. Nowacki, B. Monasse, E. Piorkowska, A. Galeski, and J. M. Haudin, "Spherulite nucleation in isotactic polypropylene based nanocomposites with montmorillonite under shear," *Polymer*, vol. 45, no. 14, pp. 4877–4892, 2004.

[24] J. Morawiec, A. Pawlak, M. Slouf, A. Galeski, E. Piorkowska, and N. Krasnikowa, "Preparation and properties of compatibilized LDPE/organo-modified montmorillonite nanocomposites," *European Polymer Journal*, vol. 41, no. 5, pp. 1115–1122, 2005.

[25] D. N. Bikiaris, G. Z. Papageorgiou, E. Pavlidou, N. Vouroutzis, P. Palatzoglou, and G. P. Karayannidis, "Preparation by melt mixing and characterization of isotactic polypropylene/SiO_2 nanocomposites containing untreated and surface-treated nanoparticles," *Journal of Applied Polymer Science*, vol. 100, no. 4, pp. 2684–2696, 2006.

[26] C. Carteret, "Mid- and near-infrared study of hydroxyl groups at a silica surface: H-bond effect," *The Journal of Physical Chemistry C*, vol. 113, no. 30, pp. 13300–13308, 2009.